Available online at www.sciencedirect.com
ScienceDirect
Precambrian Research 159 (2007) 117–131
Precambrian Research
www.elsevier.com/locate/precamres

Detrital zircon geochronology of Precambrian basement sequences in the Jiangnan orogen: Dating the assembly of the Yangtze and Cathaysia Blocks

Xiao-Lei Wang[a,b,*], Jin-Cheng Zhou[a], W.L. Griffin[b], Ru-Cheng Wang[a], Jian-Sheng Qiu[a], S.Y. O'Reilly[b], Xisheng Xu[a], Xiao-Ming Liu[c], Gui-Lin Zhang[d]

[a] *State Key Laboratory for Mineral Deposits Research, Department of Earth Sciences, Nanjing University, Nanjing 210093, PR China*
[b] *ARC National Key Centre for Geochemical Evolution and Metallogeny of Continents, Department of Earth and Planetary Sciences, Macquarie University, NSW 2109, Australia*
[c] *Department of Geology, Northwest University, Xi'an 710069, PR China*
[d] *Department of Resource and Environmental Engineering, Guilin Institute of Technology, Guilin 541004, PR China*

Received 3 March 2007; received in revised form 20 May 2007; accepted 7 June 2007

Abstract

In the Jiangnan orogen, a clear angular unconformity between the Precambrian basement sequences and the overlying Neoproterozoic sedimentary strata (e.g. the Danzhou/Banxi Group, younger than ca. 800 Ma) marks the collisional orogenesis (the Jinning orogeny) between the Yangtze and Cathaysia Blocks. In contrast to the upright, open folds in the Danzhou/Banxi Group, the basement sequences were deformed into high-angle tight linear and isoclinal overturned folds. It has been previously accepted that the basement sequences are of Mesoproterozoic age. However, LA-ICP–MS U–Pb dating of detrital zircons suggests that the maximum depositional age of the basement sedimentary rocks in the western part of the Jiangnan orogen (i.e. the Sibao/Lengjiaxi Group) is ca. 860 Ma. This provides a lower limit for the assembly of the Yangtze and Cathaysia Blocks. Consequently, there may be no significant (ca. 200 Ma) early Neoproterozoic sedimentary hiatus in South China. These data, combined with published dates on orogeny-related igneous rocks in the Jiangnan orogen, indicate that the Jinning orogeny took place at 860–800 Ma, significantly younger than the typical Grenvillian orogeny at 1.3–1.0 Ga. The Sibao/Lengjiaxi Group may have been deposited in a foreland basin. The Yangtze Block and the arc terrains that resulted from the early subduction along the Jiangnan orogen might be the two main source regions for the sedimentary rocks.

Keywords: Detrital zircon geochronology; LA-ICP–MS; Terrane assembly; Yangtze; Cathaysia

1. Introduction

The timing of the assembly of paleo-continental blocks and the accompanying orogenic processes are key issues for understanding the evolution of supercontinents throughout Earth history (e.g. Condie, 2002). In the last decade, the Rodinia supercontinent, which formed primarily along Grenville-age orogens, has received

* Corresponding author. Tel.: +86 25 83686336; fax: +86 25 83686016.
E-mail address: xlwangnju@yahoo.com.cn (X.-L. Wang).

0301-9268/$ – see front matter © 2007 Elsevier B.V. All rights reserved.
doi:10.1016/j.precamres.2007.06.005

considerable attention (Hoffman et al., 1998; Meert and Powell, 2001; Torsvik, 2003). However, the exact geometry of the supercontinent is still poorly defined (Meert and Torsvik, 2003), and the amalgamations of different continental blocks might be asynchronous (e.g. Condie, 2002). In particular, the collisions between some relatively minor blocks, like Yangtze–Cathaysia, probably took place later than the main phase of Grenvillian orogenesis (Condie, 2002; Li, 1999; Zhao and Cawood, 1999; Wang et al., 2006), and they can provide useful information about the final amalgamation of the Rodinia supercontinent.

It has been generally accepted that the Jinning orogeny (or "Sibao orogeny" of some authors, e.g. Greentree et al., 2006) has led to the assembly of the Yangtze and Cathaysia Blocks. However, timing of the assembly is still a matter of significant debate. It was originally thought to be at 1000–900 Ma based on imprecise isotopic dating results (Guo et al., 1980; Xing et al., 1992; Zhou and Zhu, 1993). A Triassic collision between the Yangtze and Cathaysia has been proposed by Hsü et al. (1988), although it has been questioned by many scholars and new geological, geochronological and geochemical studies of the igneous rocks in the Jiangnan orogen (Xing et al., 1992; Charvet et al., 1996; Li et al., 2003a,b and references therein). Later, Li (1999) considered the final amalgamation of the Yangtze and Cathaysia Blocks have taken place at ca. 820 Ma, based on more recent ages for the granites in the western end of the Jiangnan orogen. However, in recent years the formation of the middle Neoproterozoic granites of South China has been attributed to a mantle plume (Li et al., 2002, 2003a,b). At present, the timing of the Jinning orogeny is still unknown. It is considered to have taken place at 1000–900 Ma (e.g. Li et al., 2003a,b, 2005) or over a longer time period of 1000–800 Ma (e.g. Wang, 2004).

Li et al. (2002) proposed a Grenville-age metamorphic event in South China and suggested that the assembly of the Yangtze and Cathaysia Blocks could have taken place at ca. 1.0 Ga. However, these authors did not provide petrological evidence for the existence of significant Grenville-aged metamorphism and accompanying magmatism in South China. The metamorphic ages of the zircon rims provided by them cannot be regarded as compelling geochronological evidence for a Grenvillian continental collision. Perhaps more importantly, the samples they studied are all from the periphery of South China, not the interior nor from areas near the suture between the Yangtze and Cathaysia Blocks.

The Jiangnan orogen (Fig. 1a) remains the key to understanding the assembly and evolution of the Yangtze and Cathaysia Blocks. In recent years, much attention has been focused on the characteristics (i.e. orogenic or anorogenic) of the Precambrian magmatism along the Jiangnan orogen (Zhou et al., 2000, 2004; Wang et al., 2004, 2006). However, the basement sedimentary rocks have received little attention, and there have been no reliable geochronological constraints on their depositional age.

Over the last 10 years, great advances have been made in the application of laser ablation (LA)-ICP–MS U–Pb geochronology (e.g. Jackson et al., 2004). This method is appropriate to the U–Pb isotopic analysis of the detrital zircons in sedimentary rocks, and can give effective constraints on the lower age limit for deposition of the sedimentary strata (Nelson, 2001; Fedo et al., 2003). In this work, we present LA-ICP–MS U–Pb isotopic data for detrital zircons from Precambrian sedimentary rocks in the western part of the Jiangnan orogen. These dating results give new insights into the timing of assembly of the Yangtze and Cathaysia Blocks.

2. Geological setting

The Yangtze and Cathaysia Blocks, separated by the ca. 1500 km long ENE-trending (in present coordinates) Jiangnan orogen, constitute the South China Block (Fig. 1a). The Jiangnan orogen is mainly composed of Precambrian sedimentary strata and igneous rocks (Fig. 1a), and may record the convergence history of the Yangtze–Cathaysia Blocks (Charvet et al., 1996; Zhao and Cawood, 1999; Wang et al., 2006). The Precambrian sedimentary strata in the orogen basically consist of two low-grade metamorphic sequences that are separated by an angular unconformity (Fig. 2a–c). It has been generally accepted that the unconformity records a regional orogenic movement (Jinning orogeny) along the southeastern margin of the Yangtze Block (e.g. Wang and Li, 2003). The Neoproterozoic sedimentary strata above this unconformity, named the Banxi Group in Hunan Province, the Danzhou Group in northern Guangxi Province and the Dengshan Group in Jiangxi Province, are mainly composed of sandstone, slate, conglomerate, pelite and lesser carbonate, spilite and volcanoclastic rocks. The Danzhou/Banxi Group represents the lowest cover sequence overlying the basement of the Yangtze Block, and exhibits characteristics of an extensional environment (Wang and Li, 2003). The volcanic-intrusive mafic rocks in the sequences also suggest a post-orogenic extensional setting (Wang et al., in press). The structural style of the Neoproterozoic strata is relatively simple, basically with near upright, open folds (BGMRJX, 1984; BGMRGX, 1985; BGMRHN, 1988;

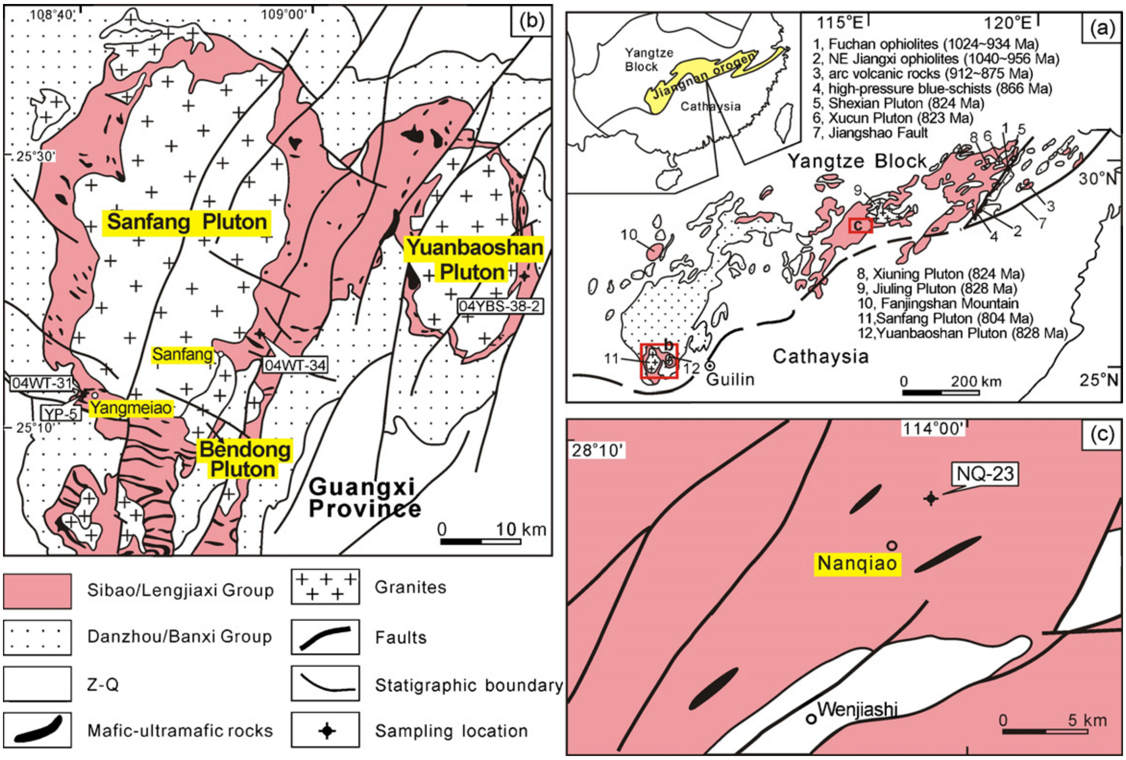

Fig. 1. Geological Sketch map of the Western part of the Jiangnan orogen (modified after BGMRHN, 1988; Zhou and Zhu, 1993; Wang, 2000; Wang et al., 2006). (a) The Jiangnan orogen; (b) northern Guangxi Province; (c) Nanqiao area of northeastern Hunan Province.

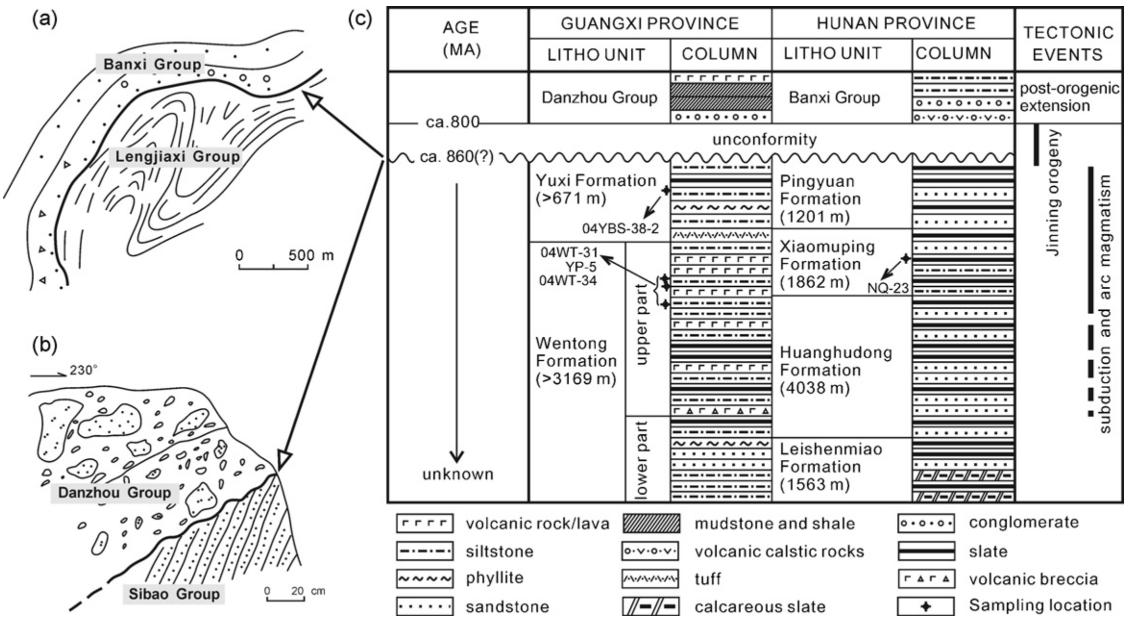

Fig. 2. Field relationships between the various strata in the Jiangnan orogen. (a) The angular unconformity between the Lengjiaxi Group and the Banxi Group (after Tang et al., 1997); (b) angular unconformity between the Sibao Group and the Danzhou Group (after GXRGST, 1995); the Sibao Group is overlain by the gravels of the lower part of the Danzhou Goup; (c) stratigraphic units of the basement sequences in the western part of the Jiangnan orogen (modified after BGMRGX, 1985; BGMRHN, 1988; Tang, 1989).

Zhou et al., 2004; Fig. 2a and b). However, the basement sequences below the unconformity, the Lengjiaxi Group (equivalent to the Sibao Group in Guangxi Province and the Shuangqiaoshan Group in Jiangxi Province; Fig. 2c), were deformed into high-angle tight linear and isoclinal overturned folds (BGMRJX, 1984; BGMRGX, 1985; BGMRHN, 1988; Zhou et al., 2004; Fig. 2a and b), in response to the Jinning orogeny. Because of the complex structures developed in the basement sequences, it is very difficult to give accurate estimates for the thickness and the order of the sequences in the field, and some of the previous estimates are listed in Fig. 2c. Basically, the basement sequences are mainly composed of dark green sandstone, siltstone, pelitic siltstone, slate, phyllite, and lesser mafic–ultramafic volcanic rocks (e.g. tholeiites, pillow spilites and volcanoclastic rocks) in some areas (Fig. 2c). They generally show depositional features of flysch turbidites (BGMRGX, 1985; BGMRHN, 1988).

These basement sequences are intruded by Neoproterozoic peraluminous granites. According to published isotopic dating of the intruding granites (e.g. a ca. 1063 Ma Rb–Sr isochron age for the Bendong granites; Fig. 1b), the Lengjiaxi Group and its equivalent sequences have been previously regarded as Mesoproterozoic. However, new LA-ICP–MS U–Pb zircon dating results give an age of 822.7 ± 3.8 Ma for the Bendong pluton (Wang et al., 2006). Apart from the ca. 960 Ma plagi-granites related to the ophiolite suites (Li et al., 1994) and the ca. 900 Ma granitoids associated with the arc magmatism in the eastern part of the orogen (Zhou, 2003), no granites with ages of 1000–900 Ma have been found in the Jiangnan orogen. These new results for the granites require us to revisit the age of the intruded basement sedimentary rocks, and to obtain more precise chronological data.

In this work, five samples from the basement sedimentary rocks of the western part of the Jiangnan orogen have been selected for analysis. Sample locations are shown in Fig. 1 and Fig. 2c. Three samples (04WT-31, 04WT-34 and YP-5) were collected from the upper part of the Wentong Formation, and one (04YBS-38-2) from the Yuxi Formation of the Sibao Group of northern Guangxi Province. The other sample (NQ-23) was collected from the Xiaomuping Formation of the Lengjiaxi Group in Hunan Province.

3. Analytical methods and data treatment

Zircon grains were separated using conventional heavy liquid and magnetic techniques, then mounted in epoxy resin and polished down to expose the grain centers. Cathodo-luminescence (CL) photos (Fig. 3) were acquired with a Mono CL3+ (Gatan, USA) attached to a scanning electron microscope (Quanta 400 FEG) at the State Key Laboratory of Continental Dynamics, Northwest University, Xi'an.

U–Pb zircon dating of three samples (04WT-34, 04YBS-38-2 and NQ-23) was carried out at the State Key Laboratory of Continental Dynamics, Northwest University. The ICP–MS instruments used were an ELAN6100 DRC from Perkin Elmer/SCIEX (Canada) with a dynamic reaction cell (DRC) and an Agillent 7500a. A GeoLas 193 nm laser-ablation system (MicroLas, Göttingen, Germany) was used for the laser-ablation analyses. Analytical processes are similar to those of Yuan et al. (2003) and Wang et al. (2006). All U–Th–Pb isotope measurements were performed using

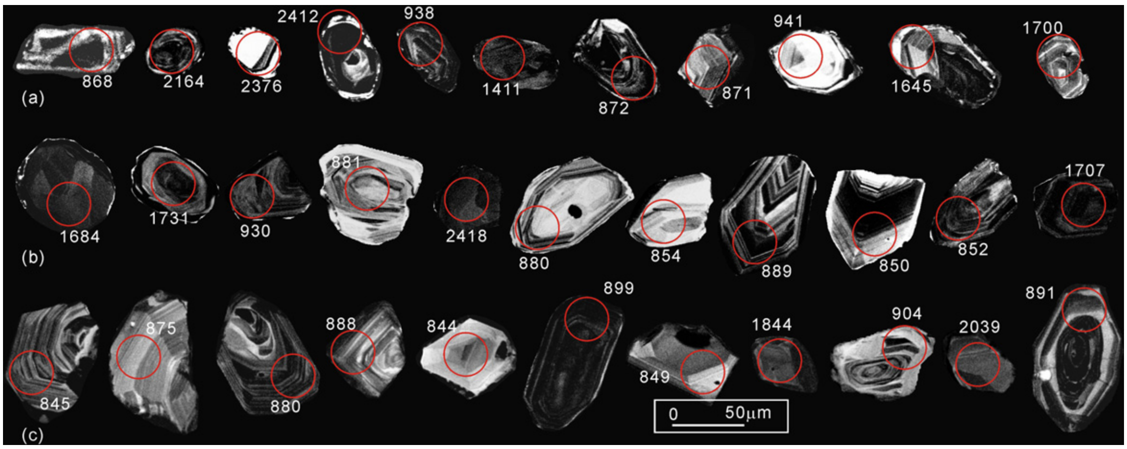

Fig. 3. Representative cathodoluminescence (CL) images of detrital zircons from the basement sedimentary rocks. (a) The Wentong Formation of the Sibao Group; (b) the Yuxi Formation of the Sibao Group; (c) the Lengjiaxi Group. Circles indicating with ages (Ma) stand for the La-ICP–MS U–Pb analysis spots.

zircon 91500 as an external standard for age calculation (Wiedenbeck et al., 1995). A spot size of 30 μm was used for all analyses. Isotopic ratios were calculated using GLITER 4.0 (van Achterbergh et al., 2001) while common lead correction was carried out using the EXCEL program ComPbCorr#_151 (Andersen, 2002).

In order to check the validity of the U–Pb dating results from Northwest University, some zircon grains of sample 04YBS-38-2 and NQ-23 and two new samples (04WT-31 and YP-5) were analyzed in the GEMOC Key Centre, using an Agilent 7500s ICP–MS attached to a New Wave 213 nm laser ablation system with an in-house sample cell. Detailed analytical procedures are similar to those described by Griffin et al. (2004) and Jackson et al. (2004). U–Pb fractionation was corrected using zircon standard GEMOC GJ-1 ($^{207}Pb/^{206}Pb$ age of 608.5 ± 1.5 Ma, Jackson et al., 2004) and accuracy was controlled using zircon standards 91500 ($^{207}Pb/^{206}Pb$ age of 1065.4 ± 0.6 Ma, Wiedenbeck et al., 1995) and Mud Tank (intercept age of 732 ± 5 Ma, Black and Gulson, 1978). Samples were analyzed in runs of ca. 18 analyses which included six zircon standards and up to 12 sample points. Most analyses were carried out using a beam with a 30 μm diameter and a repetition rate of 4 Hz. U–Pb ages were calculated from the raw signal data using the on-line software package GLITTER (ver. 4.4) (www.mq.edu.au/GEMOC). Because ^{204}Pb could not be measured due to low signal and interference from ^{204}Hg in the gas supply, common lead correction was carried out using the EXCEL program ComPbCorr#3_15G (Andersen, 2002). The analytical results from GEMOC are generally in agreement within error with those from Northwest University (China), suggesting the results of this work are reliable.

All of the U–Th–Pb age calculations and plotting of concordia diagrams were done using the ISOPLOT/Ex program (ver. 2.06) of Ludwig (1999). Unless otherwise stated, the age data shown in the figures and subsequent discussions are based on $^{207}Pb/^{206}Pb$ ages for grains older than 1.0 Ga, and $^{206}Pb/^{238}U$ ages for younger grains. Zircon U–Pb isotopic compositions are presented in Table 1

. Uncertainties on individual analyses in the data table and concordia plots are presented as 1σ.

4. Results

4.1. Wentong Formation, Sibao Group

Three samples (04WT-31, 04WT-34 and YP-5) were collected from the Wentong Formation, i.e. the lower part of the Sibao Group. Zircon grains separated from the formation are subhedral to rounded, with most grains less than 100 μm long, showing oscillatory zoning (Fig. 3a).

Samples 04WT-31 (N25°11′47.4″, E108°40′7.4″) and YP-5 (N25°11′46.9″, E108°40′7.2″) are sandstones collected near the Yangmeiao village in northern Guangxi Province (Fig. 1b). In the area, the Sibao Group was intruded by the Yangmeiao mafic-ultramafic rocks (828 ± 7 Ma, Li et al., 1999) (Fig. 4a) and is overlain by the Neoproterozoic Danzhou Group (Fig. 4a and b). All of the analyses plot on or near Concordia and define three age populations: 2.6–2.5 Ga, 1.8–1.6 Ga and 1.0–0.86 Ga (Fig. 5a and b). A few analyses show ages of ca. 2.1 Ga or within the range of 1.4–1.1 Ga. The youngest ages of the two samples are close to 860 Ma. 10 analyses of zircons from YP-5 yield an intercept age

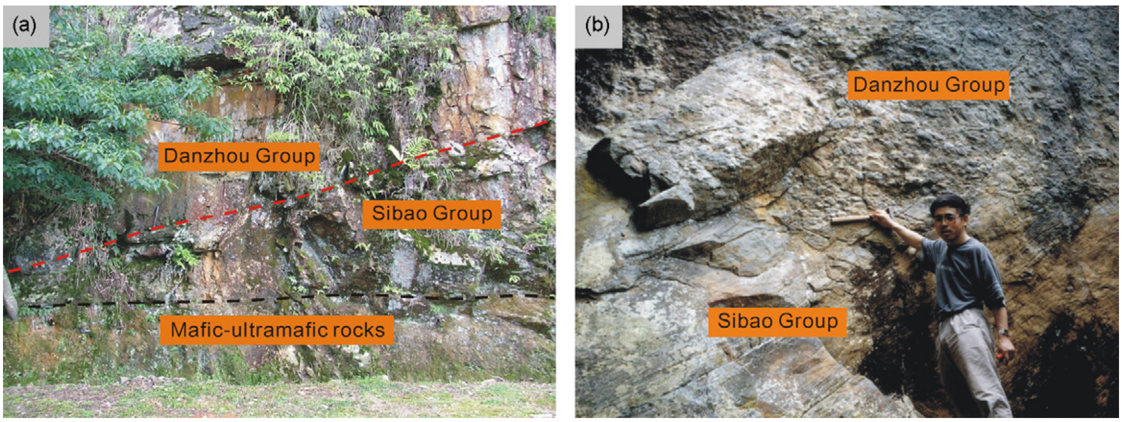

Fig. 4. Field relationship between the Danzhou Group and the Sibao Group. (a) Picture of the outcrop near the Yangmeiao village, where the Sibao Group is unconformably overlain by basal conglomerates of the Danzhou Group, and is intruded by the ca. 828 Ma mafic-ultramafic rocks; (b) picture of the outcrop near the Jiuxiao village, where the Sibao Group is unconformably overlain by basal conglomerates of the Danzhou Group.

Table 1
Laser ablation ICP–MS U–Pb analyses for the detrital zircons from the sedimentary rocks of the Jiangnan orogen

Analysis	Isotopic ratios						Isotopic ages (Ma)						Disc. (%)	Correction type
	^{207}Pb/^{206}Pb	1σ	^{207}Pb/^{235}U	1σ	^{206}Pb/^{238}U	1σ	^{207}Pb/^{206}Pb	1σ	^{207}Pb/^{235}U	1σ	^{206}Pb/^{238}U	1σ		
Sample 04WT-31														
WT01	0.1690	0.0020	11.469	0.129	0.4924	0.0048	2547	8	2562	10	2581	21	1.6	None
WT02	0.1135	0.0015	5.272	0.066	0.3371	0.0035	1856	10	1864	11	1872	17	1	None
WT03	0.1678	0.0020	11.161	0.130	0.4825	0.0048	2536	9	2537	11	2538	21	0.1	None
WT04	0.0799	0.0010	2.289	0.028	0.2077	0.0020	1195	11	1209	9	1217	11	2	None
WT05	0.1777	0.0029	12.299	0.200	0.5022	0.0059	2631	13	2628	15	2623	25	−0.4	None
WT06	0.0691	0.0012	1.417	0.024	0.1489	0.0017	901	17	896	10	895	10	−0.8	None
WT07	0.0986	0.0012	3.816	0.043	0.2806	0.0028	1599	10	1596	9	1594	14	−0.3	None
WT08	0.0711	0.0008	1.608	0.018	0.1641	0.0016	959	10	973	7	980	9	2.3	None
WT09	0.1050	0.0012	4.527	0.052	0.3127	0.0031	1714	9	1736	9	1754	15	2.7	None
WT10	0.0798	0.0011	2.280	0.029	0.2073	0.0021	1191	12	1206	9	1215	11	2.2	None
WT11	0.1619	0.0021	10.722	0.129	0.4804	0.0045	2475	9	2499	11	2529	20	2.6	None
WT12	0.0679	0.0011	1.365	0.020	0.1459	0.0015	864	15	874	9	878	8	1.7	None
WT13	0.0684	0.0009	1.357	0.018	0.1440	0.0015	879	13	870	8	867	8	−1.5	None
WT14	0.1098	0.0014	4.902	0.061	0.3239	0.0033	1795	10	1803	10	1809	16	0.9	None
WT15	0.0707	0.0010	1.611	0.023	0.1652	0.0017	950	14	974	9	986	9	4.1	None
WT16	0.0674	0.0009	1.312	0.017	0.1411	0.0014	851	12	851	7	851	8	0	None
WT17	0.0681	0.0018	1.329	0.034	0.1415	0.0018	872	32	858	15	853	10	−2.3	None
WT18	0.1650	0.0021	10.662	0.129	0.4687	0.0047	2508	9	2494	11	2478	21	−1.4	None
WT19	0.0860	0.0010	2.784	0.033	0.2347	0.0024	1339	10	1351	9	1359	12	1.7	None
WT20	0.0679	0.0008	1.386	0.017	0.1480	0.0015	866	11	883	7	889	9	2.8	None
WT21	0.0680	0.0008	1.353	0.016	0.1443	0.0015	868	11	869	7	869	8	0.2	None
WT22	0.0721	0.0009	1.622	0.019	0.1631	0.0016	989	11	979	7	974	9	−1.6	None
WT23	0.0680	0.0009	1.333	0.017	0.1422	0.0015	869	12	860	8	857	8	−1.5	None
WT25	0.0727	0.0009	1.687	0.020	0.1685	0.0017	1004	11	1004	8	1004	9	−0.1	None
WT26	0.1626	0.0027	10.694	0.173	0.4770	0.0056	2483	13	2497	15	2514	24	1.5	None
WT27	0.0682	0.0009	1.391	0.018	0.1479	0.0015	876	12	885	8	889	8	1.7	None
WT28	0.0679	0.0008	1.378	0.016	0.1472	0.0015	866	11	880	7	885	8	2.4	None
WT29	0.0679	0.0014	1.340	0.025	0.1431	0.0015	866	22	863	11	862	9	−0.5	None
WT30	0.0870	0.0012	2.825	0.037	0.2355	0.0025	1361	12	1362	10	1363	13	0.1	None
WT31	0.0679	0.0010	1.351	0.019	0.1444	0.0015	866	14	868	8	869	8	0.5	None
WT32	0.0676	0.0009	1.361	0.017	0.1460	0.0015	857	12	872	7	879	9	2.6	None
WT33	0.0684	0.0018	1.340	0.035	0.1421	0.0020	882	31	863	15	856	11	−3.1	None
WT34	0.0730	0.0011	0.025	0.1673	0.1673	0.0019	1013	14	1002	10	997	10	−1.7	None
WT35	0.0741	0.0025	0.056	0.1626	0.1626	0.0027	1043	41	993	21	971	15	−7.4	None
WT36	0.0697	0.0012	0.025	0.1463	0.1463	0.0018	920	18	891	11	880	10	−4.7	None
WT38	0.1643	0.0030	10.152	0.187	0.4481	0.0057	2501	15	2449	17	2387	25	−5.5	None
WT39	0.1118	0.0016	5.116	0.074	0.3318	0.0038	1830	12	1839	12	1847	18	1.1	None
WT40	0.1090	0.0017	4.921	0.076	0.3276	0.0039	1782	13	1806	13	1827	19	2.9	None
WT41	0.1143	0.0016	5.303	0.077	0.3366	0.0039	1868	12	1869	12	1870	19	0.1	None
WT42	0.0770	0.0011	1.996	0.027	0.1880	0.0020	1122	12	1114	9	1110	11	−1.1	None
WT43	0.1656	0.0022	10.819	0.144	0.4740	0.0052	2513	10	2508	12	2501	23	−0.6	None
WT44	0.1654	0.0025	10.860	0.164	0.4763	0.0055	2512	12	2511	14	2511	24	0	None
WT45	0.0871	0.0012	2.924	0.041	0.2435	0.0027	1362	13	1388	11	1405	14	3.5	None
WT47	0.0776	0.0014	2.156	0.039	0.2015	0.0025	1137	18	1167	13	1183	13	4.5	None
WT48	0.0875	0.0010	2.830	0.032	0.2345	0.0024	1372	10	1364	9	1358	12	−1.1	None
WT49	0.1670	0.0019	10.970	0.120	0.4764	0.0048	2528	8	2521	10	2511	21	−0.8	None
WT50	0.1134	0.0014	5.099	0.062	0.3262	0.0035	1854	10	1836	10	1820	17	−2.1	None
WT52	0.0878	0.0014	2.889	0.045	0.2387	0.0028	1378	14	1379	12	1380	15	0.2	None
WT53	0.0690	0.0010	1.378	0.018	0.1448	0.0015	899	13	879	8	872	8	−3.3	None
WT54	0.0673	0.0013	1.307	0.024	0.1408	0.0016	848	20	849	11	849	9	0.1	None
Sample YP-5														
YP01	0.1038	0.0019	4.188	0.063	0.2928	0.0030	1692	34	1672	12	1655	15	−2.5	Disc
YP02	0.1100	0.0026	4.811	0.103	0.3171	0.0032	1800	44	1787	18	1776	16	−1.6	Disc
YP03	0.2071	0.0050	15.972	0.344	0.5594	0.0061	2883	40	2875	21	2864	25	−0.8	Disc
YP04	0.0680	0.0015	1.317	0.030	0.1405	0.0020	869	25	853	13	847	11	−2.7	None
YP05	0.1639	0.0027	10.473	0.141	0.4635	0.0046	2496	29	2478	12	2455	20	−2.0	Disc
YP06	0.0675	0.0013	1.319	0.026	0.1418	0.0019	852	20	854	11	855	11	0.4	None
YP07	0.1163	0.0026	5.356	0.119	0.3342	0.0047	1899	21	1878	19	1859	23	−2.5	None
YP08	0.0709	0.0014	1.401	0.027	0.1434	0.0019	954	20	889	12	864	11	−10.1	None
YP09	0.0706	0.0021	1.539	0.043	0.1582	0.0021	945	36	946	17	947	12	0.2	None
YP10	0.0985	0.0019	3.786	0.072	0.2789	0.0036	1596	18	1590	15	1586	18	−0.7	None

Table 1 (*Continued*)

Analysis	Isotopic ratios						Isotopic ages (Ma)						Disc. (%)	Correction type
	$^{207}Pb/^{206}Pb$	1σ	$^{207}Pb/^{235}U$	1σ	$^{206}Pb/^{238}U$	1σ	$^{207}Pb/^{206}Pb$	1σ	$^{207}Pb/^{235}U$	1σ	$^{206}Pb/^{238}U$	1σ		
YP11	0.0680	0.0014	1.357	0.026	0.1447	0.0015	868	23	870	11	871	9	0.4	None
YP12	0.0682	0.0012	1.360	0.022	0.1447	0.0015	875	17	872	9	871	9	−0.5	None
YP13	0.1128	0.0016	5.057	0.070	0.3252	0.0035	1845	12	1829	12	1815	17	−1.8	None
YP14	0.1010	0.0014	3.852	0.051	0.2768	0.0027	1642	12	1604	11	1575	14	−4.6	None
YP15	0.0703	0.0020	1.467	0.041	0.1514	0.0021	937	34	917	17	909	12	−3.2	None
YP16	0.0969	0.0017	3.620	0.049	0.2710	0.0028	1565	33	1554	11	1546	14	−1.4	Disc
YP17	0.0681	0.0012	1.349	0.024	0.1437	0.0018	872	18	867	10	865	10	−0.8	None
YP19	0.0998	0.0017	3.873	0.066	0.2815	0.0034	1621	15	1608	14	1599	17	−1.6	None
YP20	0.1562	0.0034	9.775	0.187	0.4538	0.0049	2415	38	2414	18	2412	22	−0.1	Disc
YP21	0.0713	0.0011	1.511	0.021	0.1537	0.0016	967	14	935	8	922	9	−5	None
YP23	0.1652	0.0024	10.691	0.156	0.4696	0.0052	2509	11	2497	14	2482	23	−1.3	None
YP24	0.0706	0.0009	1.515	0.020	0.1556	0.0016	947	12	937	8	932	9	−1.6	None
YP25	0.0716	0.0010	1.558	0.022	0.1578	0.0017	975	13	954	9	945	9	−3.3	None
YP26	0.0685	0.0011	1.362	0.021	0.1442	0.0016	883	15	873	9	868	9	−1.8	None
YP27	0.0710	0.0010	1.577	0.022	0.1611	0.0018	957	13	961	9	963	10	0.7	None
YP28	0.1623	0.0034	10.294	0.179	0.4600	0.0053	2480	36	2462	16	2440	23	−1.9	Disc
YP29	0.1002	0.0013	3.880	0.047	0.2808	0.0028	1629	10	1610	10	1595	14	−2.3	None
YP30	0.1324	0.0017	7.175	0.089	0.3931	0.0041	2130	10	2133	11	2137	19	0.4	None
YP31	0.0999	0.0013	3.935	0.050	0.2856	0.0029	1623	11	1621	10	1619	15	−0.3	None
YP32	0.1638	0.0027	10.669	0.178	0.4723	0.0057	2496	14	2495	15	2494	25	−0.1	None
YP33	0.1003	0.0014	4.006	0.053	0.2897	0.0030	1630	11	1635	11	1640	15	0.7	None
YP34	0.0675	0.0010	1.330	0.018	0.1429	0.0015	854	14	859	8	861	8	0.8	None
YP35	0.1054	0.0012	4.553	0.052	0.3133	0.0032	1721	9	1741	10	1757	16	2.4	None
YP36	0.0903	0.0017	2.925	0.050	0.2350	0.0026	1431	17	1388	13	1361	14	−5.5	None
YP37	0.0676	0.0009	1.324	0.017	0.1420	0.0015	858	12	856	8	856	8	−0.2	None
YP38	0.1055	0.0013	4.561	0.055	0.3136	0.0033	1723	10	1742	10	1758	16	2.3	None
YP39	0.0846	0.0011	2.606	0.033	0.2233	0.0023	1307	11	1302	9	1299	12	−0.7	None
YP40	0.1135	0.0016	5.120	0.068	0.3272	0.0033	1857	11	1839	11	1825	16	−2	None
YP41	0.1348	0.0017	7.261	0.091	0.3907	0.0040	2161	10	2144	11	2126	19	−1.9	None
YP42	0.1769	0.0029	11.755	0.176	0.4821	0.0051	2624	12	2585	14	2536	22	−4	None
YP43	0.0715	0.0010	1.569	0.021	0.1593	0.0017	971	13	958	8	953	9	−2	None
YP44	0.1051	0.0014	4.423	0.058	0.3054	0.0032	1715	11	1717	11	1718	16	0.2	None
YP45	0.1654	0.0023	10.818	0.143	0.4743	0.0049	2512	10	2508	12	2502	21	−0.5	None
YP46	0.0675	0.0012	1.318	0.023	0.1417	0.0017	853	18	854	10	854	10	0.1	None
Sample 04WT-34														
W01	0.1184	0.0024	4.827	0.046	0.2957	0.0028	1932	8	1790	8	1670	14	−15.4	None
W02	0.0933	0.0016	2.937	0.041	0.2283	0.0022	1494	33	1391	11	1326	12	−12.4	Disc
W03	0.1617	0.0032	9.388	0.089	0.4212	0.0040	2473	7	2377	9	2266	18	−9.9	None
W04	0.0690	0.0014	1.371	0.024	0.1442	0.0014	898	42	877	10	868	8	−3.5	Disc
W05	0.1045	0.0022	3.514	0.063	0.2438	0.0025	1706	39	1530	14	1406	13	−19.5	Disc
W07	0.1063	0.0020	3.516	0.054	0.2400	0.0024	1736	34	1531	12	1386	13	−22.4	Disc
W08	0.1350	0.0021	6.161	0.074	0.3311	0.0032	2164	28	1999	10	1843	16	−17	Disc
W09	0.1083	0.0021	2.666	0.044	0.1786	0.0018	1771	36	1319	12	1059	10	−43.5	Disc
W10	0.1049	0.0021	4.034	0.068	0.2789	0.0029	1713	37	1641	14	1586	14	−8.4	Disc
W11	0.0902	0.0018	2.619	0.028	0.2106	0.0020	1430	9	1306	8	1232	11	−15.2	None
W13	0.1527	0.0024	7.236	0.087	0.3438	0.0034	2376	27	2141	11	1905	16	−22.9	Disc
W17	0.1560	0.0031	8.393	0.082	0.3903	0.0038	2412	8	2274	9	2124	17	−14	None
W20	0.0856	0.0017	2.149	0.022	0.1822	0.0018	1328	9	1165	7	1079	10	−20.4	None
W23	0.1038	0.0023	3.923	0.077	0.2741	0.0029	1694	42	1618	16	1561	15	−8.8	Disc
W24	0.0718	0.0017	1.551	0.033	0.1566	0.0016	981	49	951	13	938	9	−4.8	Disc
W25	0.1139	0.0024	4.656	0.084	0.2966	0.0031	1862	38	1759	15	1674	15	−11.4	Disc
W26	0.0893	0.0018	2.470	0.024	0.2006	0.0019	1411	8	1263	7	1178	10	−18	None
W28	0.0702	0.0015	1.403	0.016	0.1449	0.0014	935	10	890	7	872	8	−7.2	None
W29	0.0694	0.0015	1.383	0.017	0.1446	0.0014	909	12	882	7	871	8	−4.6	Disc
W30	0.0712	0.0018	1.542	0.035	0.1571	0.0016	962	52	947	14	941	9	−2.4	Disc
W31	0.0917	0.0023	2.500	0.057	0.1978	0.0021	1460	49	1272	17	1164	11	−22.2	Disc
W32	0.0692	0.0016	1.465	0.030	0.1535	0.0016	905	48	916	12	921	9	1.8	Disc
W35	0.1011	0.0020	3.467	0.034	0.2487	0.0024	1645	8	1520	8	1432	12	−14.4	None
W36	0.1042	0.0022	3.400	0.064	0.2368	0.0025	1700	40	1504	15	1370	13	−21.5	Disc
W39	0.0944	0.0019	3.343	0.033	0.2568	0.0025	1517	8	1491	8	1473	13	−3.2	None
W41	0.1057	0.0019	3.909	0.056	0.2682	0.0027	1726	33	1616	12	1532	14	−12.7	Disc
W42	0.1569	0.0031	8.116	0.078	0.3753	0.0036	2422	7	2244	9	2054	17	−17.7	None
W43	0.1288	0.0026	5.922	0.057	0.3336	0.0032	2081	8	1964	8	1856	15	−12.5	None
W45	0.1014	0.0020	3.608	0.035	0.2581	0.0025	1650	8	1551	8	1480	13	−11.6	None

Table 1 (*Continued*)

Analysis	Isotopic ratios						Isotopic ages (Ma)						Disc. (%)	Correction type
	$^{207}Pb/^{206}Pb$	1σ	$^{207}Pb/^{235}U$	1σ	$^{206}Pb/^{238}U$	1σ	$^{207}Pb/^{206}Pb$	1σ	$^{207}Pb/^{235}U$	1σ	$^{206}Pb/^{238}U$	1σ		
W46	0.1663	0.0033	10.898	0.104	0.4753	0.0046	2521	7	2514	9	2507	20	−0.7	None
W47	0.1134	0.0016	4.719	0.050	0.3019	0.0029	1854	26	1771	9	1701	14	−9.4	Disc
W48	0.1106	0.0018	4.597	0.061	0.3014	0.0030	1809	31	1749	11	1698	15	−7	Disc
Sample 04YBS-38-2														
Y-1	0.1123	0.0023	3.890	0.039	0.2512	0.0024	1838	8	1612	8	1444	13	−23.9	None
Y-3	0.0982	0.0020	3.690	0.035	0.2725	0.0026	1591	8	1569	8	1553	13	−2.7	None
Y-4	0.1368	0.0024	5.280	0.075	0.2799	0.0028	2188	31	1866	12	1591	14	−30.7	Disc
Y-5	0.1561	0.0022	8.200	0.082	0.3810	0.0036	2414	24	2253	9	2081	17	−16.1	Disc
Y-6[a]	0.1043	0.0023	4.295	0.093	0.2985	0.0040	1703	41	1692	18	1684	20	−1.2	None
Y-7[a]	0.1307	0.0036	6.945	0.188	0.3855	0.0056	2107	49	2104	24	2102	26	−0.3	None
Y-8	0.1086	0.0022	4.612	0.048	0.3081	0.0030	1776	8	1751	9	1731	15	−2.9	None
Y-9	0.1767	0.0035	11.388	0.109	0.4674	0.0045	2622	7	2555	9	2472	20	−6.9	None
Y-10	0.0713	0.0015	1.527	0.018	0.1553	0.0015	966	11	941	7	930	9	−4.0	None
Y-11	0.0996	0.0020	3.899	0.037	0.2839	0.0027	1617	8	1614	8	1611	14	−0.4	None
Y-13	0.0684	0.0014	1.381	0.015	0.1464	0.0014	881	10	881	6	881	8	−0.1	None
Y-14	0.1620	0.0032	10.164	0.097	0.4552	0.0044	2476	7	2450	9	2418	19	−2.8	None
Y-15	0.1015	0.0014	2.558	0.027	0.1828	0.0017	1652	27	1289	8	1082	9	−37.4	Disc
Y-16	0.0686	0.0014	1.402	0.014	0.1482	0.0014	887	9	890	6	891	8	0.5	None
Y-17	0.0682	0.0019	1.375	0.035	0.1462	0.0015	875	58	878	15	880	9	0.6	Disc
Y-18	0.0837	0.0021	2.274	0.052	0.1972	0.0021	1284	50	1204	16	1160	11	−10.6	Disc
Y-19[a]	0.0991	0.0023	3.791	0.084	0.2774	0.0037	1608	44	1591	18	1578	19	−2.1	None
Y-20	0.0703	0.0014	1.384	0.014	0.1429	0.0014	937	9	882	6	861	8	−8.7	None
Y-21	0.1090	0.0022	4.684	0.045	0.3119	0.0030	1782	8	1764	8	1750	15	−2.1	None
Y-23	0.1621	0.0026	9.225	0.117	0.4127	0.0041	2478	28	2361	12	2227	19	−12	Disc
Y-24	0.0712	0.0014	1.445	0.014	0.1473	0.0014	962	9	908	6	886	8	−8.5	None
Y-25	0.0976	0.0019	3.411	0.033	0.2536	0.0024	1578	8	1507	8	1457	12	−8.6	None
Y-26	0.1056	0.0016	3.436	0.040	0.2360	0.0023	1725	29	1513	9	1366	12	−23.1	Disc
Y-27	0.0728	0.0014	1.725	0.017	0.1720	0.0017	1007	9	1018	6	1023	9	1.7	None
Y-29	0.0674	0.0013	1.328	0.013	0.1429	0.0014	851	9	858	6	861	8	1.2	None
Y-30	0.0683	0.0014	1.335	0.015	0.1417	0.0014	878	11	861	7	854	8	−2.9	None
Y-31[a]	0.0688	0.0014	1.398	0.029	0.1475	0.0020	892	44	888	12	887	11	−0.6	None
Y-32	0.0674	0.0013	1.374	0.014	0.1478	0.0014	851	9	878	6	889	8	4.7	None
Y-33	0.0684	0.0017	1.329	0.024	0.1409	0.0015	882	20	859	10	850	9	−3.9	None
Y-34	0.0818	0.0016	2.221	0.037	0.1968	0.0020	1242	39	1188	12	1158	11	−7.3	Disc
Y-35	0.0995	0.0020	3.900	0.037	0.2843	0.0027	1615	8	1614	8	1613	14	−0.2	None
Y-36	0.0680	0.0014	1.323	0.014	0.1412	0.0014	867	10	856	6	852	8	−2	None
Y-39[a]	0.1048	0.0015	4.380	0.064	0.3032	0.0035	1711	27	1709	12	1707	17	−0.3	None
Y-40	0.1125	0.0022	4.915	0.049	0.3170	0.0031	1840	8	1805	8	1775	15	−4	None
Y-41	0.1499	0.0030	7.776	0.074	0.3764	0.0036	2344	7	2205	9	2059	17	−14.2	None
Y-42	0.1042	0.0021	4.531	0.044	0.3154	0.0030	1701	8	1737	8	1767	15	4.5	None
Y-43	0.1066	0.0021	4.476	0.044	0.3047	0.0030	1741	8	1727	8	1715	15	−1.8	None
Y-44	0.1087	0.0020	4.530	0.070	0.3024	0.0031	1777	34	1737	13	1703	15	−4.7	Disc
Y-45	0.0677	0.0014	1.318	0.013	0.1412	0.0014	861	10	854	6	851	8	−1.2	None
Y-46	0.0714	0.0014	1.586	0.016	0.1612	0.0016	968	9	965	6	963	9	−0.5	None
Y-47	0.1602	0.0032	10.341	0.098	0.4684	0.0045	2458	7	2466	9	2476	20	0.9	None
Y-48	0.0704	0.0014	1.526	0.015	0.1572	0.0015	941	9	941	6	941	8	0	None
Y-49	0.1640	0.0032	10.533	0.100	0.4660	0.0045	2497	7	2483	9	2466	20	−1.5	None
Y-50	0.1282	0.0026	6.497	0.064	0.3676	0.0036	2074	8	2045	9	2018	17	−3.2	None
Y-A1[a]	0.1602	0.0023	10.028	0.144	0.4540	0.0052	2458	25	2437	13	2413	23	−2.2	None
Y-A2[a]	0.1605	0.0022	9.049	0.120	0.4089	0.0043	2461	24	2343	12	2210	19	−12.1	None
Y-A3[a]	0.0700	0.0018	1.439	0.036	0.1491	0.0022	930	54	905	15	896	12	−3.9	None
Y-A4[a]	0.1605	0.0042	3.829	0.097	0.1732	0.0024	2460	46	1599	20	1029	13	−62.8	None
Y-A5[a]	0.1860	0.0032	13.407	0.0236	0.5228	0.0065	2707	29	2709	17	2711	28	0.1	None
Y-A7[a]	0.1864	0.0027	13.339	0.179	0.5192	0.0051	2710	24	2704	13	2696	22	−0.7	None
Y-A8[a]	0.1279	0.0016	6.610	0.080	0.3749	0.0038	2069	22	2061	11	2053	18	−0.9	None
Y-A9[a]	0.1129	0.0017	5.158	0.076	0.3314	0.0037	1847	28	1846	13	1845	18	−0.1	None
Y-A10[a]	0.1613	0.0023	8.703	0.118	0.3913	0.0041	2469	24	2307	12	2129	19	−16.2	None
Y-A12[a]	0.0686	0.0010	1.373	0.018	0.1452	0.0015	886	29	877	8	874	8	−1.4	None
Sample NQ-23														
N-1	0.0985	0.0020	3.838	0.038	0.2825	0.0028	1596	8	1601	8	1604	14	0.5	None
N-2	0.0678	0.0019	1.309	0.033	0.1401	0.0015	862	58	850	14	845	8	−2.1	Disc
N-03[a]	0.0694	0.0034	1.392	0.065	0.1454	0.0019	911	102	885	28	875	11	−4.2	Disc
N-4	0.0679	0.0014	1.369	0.014	0.1463	0.0014	865	9	876	6	880	8	1.9	None

Table 1 (*Continued*)

Analysis	Isotopic ratios						Isotopic ages (Ma)						Disc. (%)	Correction type
	$^{207}Pb/^{206}Pb$	1σ	$^{207}Pb/^{235}U$	1σ	$^{206}Pb/^{238}U$	1σ	$^{207}Pb/^{206}Pb$	1σ	$^{207}Pb/^{235}U$	1σ	$^{206}Pb/^{238}U$	1σ		
N-5	0.0702	0.0014	1.431	0.015	0.1478	0.0015	935	9	902	6	888	8	−5.3	None
N-6	0.0675	0.0014	1.313	0.014	0.1411	0.0014	853	10	852	6	851	8	−0.2	None
N-8	0.1017	0.0024	3.437	0.071	0.2452	0.0027	1655	44	1513	16	1414	14	−16.2	Disc
N-10	0.0671	0.0040	1.295	0.074	0.1400	0.0019	841	126	844	33	844	11	0.4	Disc
N-13[a]	0.0689	0.0010	1.421	0.019	0.1497	0.0015	895	31	898	8	899	8	0.5	None
N-14	0.0701	0.0020	1.360	0.036	0.1407	0.0015	931	60	872	15	849	9	−9.4	Disc
N-15	0.0702	0.0017	1.370	0.029	0.1415	0.0015	935	50	876	13	853	9	−9.3	Disc
N-16	0.1685	0.0033	11.062	0.107	0.4760	0.0046	2543	7	2528	9	2510	20	−1.6	None
N-17	0.1022	0.0020	4.304	0.043	0.3055	0.0030	1664	8	1694	8	1718	15	3.7	None
N-18	0.1105	0.0024	5.198	0.070	0.3411	0.0036	1807	11	1852	11	1892	17	5.4	None
N-19	0.0709	0.0021	1.385	0.033	0.1423	0.0017	955	29	882	14	857	10	−11.3	None
N-21	0.0959	0.0019	3.552	0.037	0.2687	0.0026	1545	9	1539	8	1534	13	−0.8	None
N-22	0.0800	0.0016	2.251	0.023	0.2042	0.0020	1196	9	1197	7	1198	11	0.2	None
N-23	0.1054	0.0021	4.470	0.045	0.3076	0.0030	1721	8	1725	8	1729	15	0.5	None
N-25	0.1156	0.0023	5.409	0.054	0.3394	0.0033	1889	8	1886	8	1884	16	−0.3	None
N-26	0.1124	0.0020	5.131	0.073	0.3312	0.0033	1838	32	1841	12	1844	16	0.4	Disc
N-27	0.0686	0.0014	1.390	0.025	0.1471	0.0015	885	44	885	11	885	8	−0.1	Disc
N-28	0.1094	0.0022	4.784	0.047	0.3170	0.0031	1790	8	1782	8	1775	15	−0.9	None
N-29	0.0693	0.0021	1.370	0.038	0.1434	0.0016	907	63	876	16	864	9	−5.1	Disc
N-30	0.0722	0.0016	1.462	0.019	0.1468	0.0015	992	12	915	8	883	8	−11.7	None
N-31	0.1033	0.0021	4.303	0.041	0.3022	0.0029	1683	8	1694	8	1702	14	1.3	None
N-32[a]	0.0689	0.0009	1.430	0.017	0.1505	0.0015	897	27	902	7	904	8	0.8	None
N-33	0.0715	0.0019	1.494	0.036	0.1515	0.0016	973	55	928	15	909	9	−7	Disc
N-34	0.1089	0.0022	4.780	0.046	0.3184	0.0031	1780	8	1781	8	1782	15	0.1	None
N-37	0.1137	0.0023	5.213	0.050	0.3324	0.0032	1860	8	1855	8	1850	15	−0.6	None
N-38	0.1002	0.0020	3.900	0.040	0.2823	0.0027	1627	9	1614	8	1603	14	−1.7	None
N-39	0.0711	0.0017	1.430	0.023	0.1464	0.0016	960	17	902	10	881	9	−9.2	None
N-40	0.1260	0.0025	6.463	0.063	0.3719	0.0036	2043	8	2041	9	2039	17	−0.2	None
N-41	0.1108	0.0023	4.192	0.045	0.2745	0.0027	1812	9	1673	9	1564	14	−15.4	None
N-42	0.1130	0.0023	5.223	0.051	0.3353	0.0032	1847	8	1856	8	1864	15	1.1	None
N-46	0.1663	0.0033	10.882	0.106	0.4746	0.0046	2520	7	2513	9	2504	20	−0.8	None
N-47	0.0934	0.0016	3.383	0.049	0.2627	0.0026	1496	34	1501	11	1504	13	0.6	Disc
N-49	0.0697	0.0020	1.424	0.038	0.1482	0.0017	920	61	899	16	891	9	−3.3	Disc
N-50	0.1134	0.0023	5.136	0.049	0.3286	0.0031	1854	8	1842	8	1831	15	−1.4	None
N-A1[a]	0.0713	0.0011	1.457	0.022	0.1483	0.0016	965	33	913	9	891	9	−8.2	None
N-A2[a]	0.1329	0.0020	7.049	0.105	0.3849	0.0044	2136	27	2118	13	2099	21	−2	None
N-A3[a]	0.0685	0.0013	1.338	0.025	0.1418	0.0017	883	39	863	11	855	10	−3.5	None

Disc. (%) denotes percentage of discordance.

[a] Analyses of sample 04YBS-38-2 and NQ-23 from GEMOC.

of 859.5 ± 8.8 Ma (2σ, MSWD = 0.6). 16 analyses from sample 04WT-31 yield a similar weighted average age of 870.9 ± 6.1 Ma (2σ, 95% conf., MSWD = 1.9).

The other sample from the Wentong Formation, 04WT-34, is a siltstone located ca. 6 km east of the town of Sanfang (N25°16′13″, E108°54′10″), which makes up the country rock of the Sanfang granitic pluton (Fig. 1b). Many analyses of this sample plot below the concordia curve (Fig. 5c), probably due to Pb-loss or the existence of minor common lead. Nine analyses from this sample show $^{206}Pb/^{238}U$ ages lower than 1000 Ma; three (W04, W28 and W29) yield a weighted average age of 870.3 ± 9.1 Ma (2σ, MSWD = 0.068) which defines the maximum depositional age of the rock. One data-point (W46) plots on Concordia with a $^{207}Pb/^{206}Pb$ age of 2521 ± 7 Ma.

4.2. Yuxi Formation, Sibao Group

Sample 04YBS-38-2 is a plagioclase-quartz schist from the upper part (i.e. the Yuxi Formation) of the Sibao Group (N25°18′50″, E109°14′34″) which makes up the country rock of the Yuanbaoshan granite body (Fig. 1b). Most of the zircons from the sample are rounded and less than 100 μm across. CL images of the zircon grains from this sample show clear oscillatory zoning (Fig. 3b). Of the 54 analyses, 17 have $^{206}Pb/^{238}U$ ages lower than 1.0 Ga and plot on or close to Concordia (Fig. 5d). Of them, 12 analyses give a weighted average $^{206}Pb/^{238}U$ age of 868.2 ± 9.7 Ma (95% conf., MSWD = 3.4). The others indicate ages varying from Mesoproterozoic up to Late Archean. Two analyses yield ages of ca. 2.7 Ga.

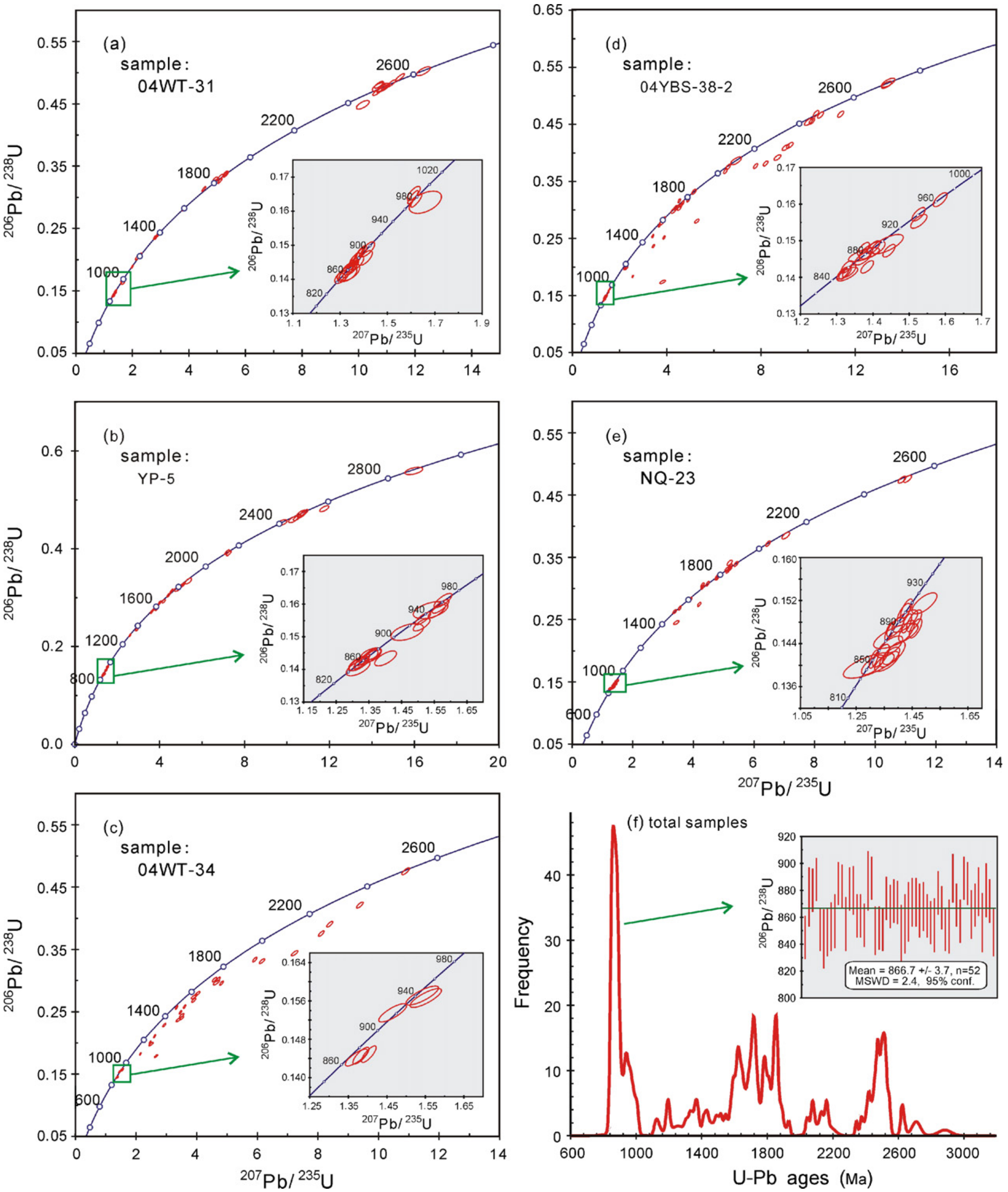

Fig. 5. Concordia plots of LA-ICP–MS U–Pb analytical results and U–Pb age histogram for the detrital zircons from the basement sedimentary sequences.

4.3. Lengjiaxi Group

Sample NQ-23 is a sandy pelite collected from the Lengjiaxi Group, located near the Nanqiao town, northeastern Hunan Province (Fig. 1c). Zircon grains separated from this sample are subhedral to rounded, and the CL images show clear oscillatory zoning (Fig. 3c). Most of the analyses of the sample plot on or near the Concordia (Fig. 5e). Of the 41 analyses, 19 yield ages lower than 1.0 Ga (Table 1; Fig. 5e). Of these, the youngest 11 analyses yield a weighted average age of 862 ± 11 Ma (2σ, 95% conf., MSWD = 3.4). An age cluster at 1.9–1.5 Ga is also evident in this sample. Two analyses yield Late Archean ages of 2543 ± 7 Ma and 2520 ± 7 Ma.

5. Discussion

5.1. Maximum depositional age of the basement sedimentary sequences

As discussed above, the basement sedimentary sequences of the Jiangnan orogen, such as the Lengjiaxi and Sibao Group, have been previously considered to be Mesoproterozoic. However, the new dating results for the detrital zircons of the sedimentary rocks show a cluster of early- to middle-Neoproterozoic ages, defining a significant peak at ca. 1000–860 Ma (Fig. 5f). Most of the Neoproterozoic zircon grains show subhedral to rounded shapes and clear oscillatory zoning (Fig. 3), excluding the possibility of metamorphic resetting or recrystallisation after their deposition. In addition, the basement sequences in the Jiangnan orogen only experienced lower-greenschist facies metamorphism, and in that environment the growth of new zircon is unlikely. Therefore, the zircons with Neoproterozoic ages in the sedimentary rocks probably are derived from a variety of igneous source rocks, and the youngest concordant ages define the maximum depositional age of the basement sedimentary sequences in the area. The mean ages (870.9 ± 6.1 Ma, 859.5 ± 8.8 Ma, 870.3 ± 9.1 Ma, 868.2 ± 9.7 Ma and 862 ± 11 Ma) of the youngest concordant detrital zircons in the above-mentioned five samples are equivalent within their uncertainties. Combining all the analyses with these young ages, a weighted average age of 866.7 ± 3.7 Ma (95% conf., MSWD = 2.4, n = 52) is obtained (Fig. 5f). This age represents our best estimate for the maximum depositional age of the basement sedimentary sequences of the Jiangnan orogen. While the lower and the upper parts of the basement sequences might represent a measurable time span, this age could at least represent the maximum age for the termination of deposition of the Sibao/Lengjiaxi Group. These new age results are quite different from those of previous studies and provide some new insights into the Precambrian evolution of South China, which are discussed below.

5.2. Time constraints on the assembly of the Yangtze and Cathaysia Blocks

One important insight from the new dating results regards the timing of the assembly of the Yangtze–Cathaysia Blocks. The amalgamation process produced the primary outline of South China. The basement sedimentary sequences in the Jiangnan orogen show tight linear folds, which are obviously older than the unconformably overlying Banxi Group. This has been regarded as important geologic evidence for the timing of the collision between the Yangtze and Cathaysia Blocks. The basement sedimentary sequences were folded due to the collision between the two blocks, which led to the unconformity between the basement strata and the later Neoproterozoic rocks (e.g. the Danzhou/Banxi Group) (BGMRJX, 1984; BGMRGX, 1985; BGMRHN, 1988; Xing et al., 1992; Zhou and Zhu, 1993). If the deposition of the basement sequences ended after ca. 860 Ma, it is clear that the assembly of the Yangtze and Cathaysia Blocks must have taken place after ca. 860 Ma. In addition, the volcanic rocks in the lower part of the Banxi Group have previously yielded an age of 814 ± 12 Ma (Wang et al., 2003) and have been re-dated at 797 ± 4 Ma (our unpublished data), which suggests that the assembly of the two blocks took place before ca. 800 Ma.

This conclusion is supported by the high-pressure metamorphic age (866 ± 14 Ma) of blueschists reported by Shu et al. (1993) in northeast Jiangxi Province, which may represent the peak of the collision between the Yangtze and Cathaysia Blocks. Similar metamorphic ages related to the orogenesis include a hornblende $^{40}Ar/^{39}Ar$ age of 844.7 ± 9.7 Ma for amphibolites near the Jiangshao Fault (Cheng, 1991), a tremolite $^{40}Ar/^{39}Ar$ age of 809 ± 36.4 Ma for an ultramafic mylonite in the northern Guangxi Province (Zhang, 2004), and a crossite $^{40}Ar/^{39}Ar$ age of 799.3 ± 9.2 Ma for an albite granite in the northeastern Jiangxi Province (Hu et al., 1993). Moreover, recently published in situ zircon U–Pb dating results (Li et al., 2003a,b; Zhong et al., 2005; Wang et al., 2006) indicate that the voluminous peraluminous granites that intrude the basement sequences in the Jiangnan orogen may have been mainly generated at 835–800 Ma. Their ages thus are close to the proposed age of the collision (ca. 860 Ma) between the Yangtze and Cathaysia Blocks. Their generation may be related to the assembly process, probably in the post-collisional stage of the orogenic processes as suggested by Wang et al. (2006). Therefore, as a whole, the Jinning orogeny leading to the assembly of the Yangtze and Cathaysia Blocks must have taken place at 860–800 Ma, clearly younger than the typical Grenville-age orogeny (1.3–1.0 Ga, McLelland et al., 1996).

The age range 1.3–1.0 Ga is very weakly represented in the detrital zircons of this study (Fig. 5f), which might suggest that Grenville-age magmatism was not significant in the area. There is currently no consensus regarding the position of the South China in the Rodinia supercontinent. The amalgamation of the main components of the Rodinia supercontinent may have taken place at 1.3–1.0 Ga (McLelland et al., 1996). The relatively young age proposed for the Jinning orogeny suggests that South China was not located in the interior of the supercontinent. Otherwise, it is difficult to understand the apparent existence of a large unclosed ocean (based on a long-lived subduction of 1000–860 Ma) between the Yangtze and Cathaysia Blocks (Zhao and Cawood, 1999; Zhou et al., 2002; Wang et al., 2006). If South China has been part of Rodinia, the final assembly of the supercontinent should have taken place at ca. 800 Ma, probably immediately followed by post-orogenic extension and/or rifting (Wang et al., 2004, in press) in the area.

5.3. Provenance and tectonic implications

Three main age peaks are evident in the detrital zircon populations of the basement sedimentary sequences of the Jiangnan orogen: 2.5–2.4 Ga, 1.8–1.6 Ga and 1.0–0.86 Ga (Fig. 5f). The former two peaks are consistent with previous estimates of the main episodes of crustal growth in South China (Li et al., 1991; Gan et al., 1996), suggesting that the zircons with these ages probably were derived from the Yangtze and/or Cathaysia Blocks. The occurrence of ca. 1.0–0.96 Ga ophiolites (Chen et al., 1991; Zhou and Zhu, 1993; Li et al., 1994) and ca. 912–875 Ma arc volcanic rocks (Cheng, 1993; Wang, 2000) in the eastern part of the Jiangnan orogen suggests that there was an ocean basin between the Yangtze and Cathaysia Blocks during the deposition of the basement sequences. Therefore, the Yangtze Block may have been a major source for the sedimentary rocks along the Jiangnan orogen, which probably provided the old (>1.0 Ga) recycled sedimentary material. Subduction-related magmatic activity at ca. 1.0–0.86 Ga is evident along the Jiangnan orogen, including the ophiolites and their related igneous rocks (Chen et al., 1991; Zhou and Zhu, 1993; Li et al., 1994) and the arc-related volcanic rocks (Cheng, 1993; Zhou and Zhu, 1993). Some inherited zircons with ages of 950–870 Ma have also been found in the 835–800 Ma peraluminous granitoids along the Jiangnan orogen (e.g. Zhong et al., 2005; Wang et al., 2006; Wu et al., 2006). Obviously, the age of the subduction-related magmatism falls in the range of the third age peak (1.0–0.86 Ga) found in the sedimentary rocks of this study. Moreover, geochemical studies on the Lengjiaxi Group indicate that a dominant component was derived from a metavolcanic–plutonic terrane (Xu et al., 2007). Therefore, it may be suggested that the Neoproterozoic arc terrains related to the subduction might be another main source for the basement sedimentary rocks. A mixture of old recycled sediments from the Yangtze Block and juvenile materials from the arc terrains could be the source of the 835–800 Ma peraluminous granitoids, this would be consistent with their isotopic features (Zhou and Wang, 1988; Wang et al., 2006; Wu et al., 2006), which are similar to those of I-type granites.

The new chronological data for the basement sedimentary sequences give us a chance to revisit the evolution of the Jiangnan orogen. Although the age of the lower part of the basement sequences is still unknown, the maximum depositional age of ca. 860 Ma for the studied samples suggests that the volcanic rocks within the sequences are probably of Neoproterozoic age, rather than being Mesoproterozoic as previously considered (Shu et al., 1995; Han et al., 1994; Wang et al., 2004). Consequently, the subduction which finally led to the formation of the Jiangnan orogen may have taken place in early Neoproterozoic time. The earliest subduction-related arc magmatism occurred at ca. 912–875 Ma (Cheng, 1993; Wang, 2000; Ye et al., 2007) in the eastern section of the Jiangnan orogen, following the formation of the 1.0–0.96 Ga ophiolites (Chen et al., 1991; Zhou and Zhu, 1993; Li et al., 1994). The arc-related magmatism in the western part of the Jiangnan orogen could be constrained by the early Neoproterozoic ages of many detrital zircons in the basement sequences (Fig. 5f), though the arc volcanic rocks have not been reported in the area. The stratigraphic studies show a continental margin depositional setting for the basement sequences (BGMRJX, 1984; BGMRGX, 1985; BGMRHN, 1988; Fig. 2c). However, the sedimentary rocks contain a great deal of materials from the arc terrains, and their maximum depositional age is close to the collision (ca. 860 Ma) along the Jiangnan orogen; they thus show similarities to sediments in typical foreland basins. To clarify the tectonic setting of the basement sequences, further stratigraphic and geochemical studies on the sedimentary rocks are needed.

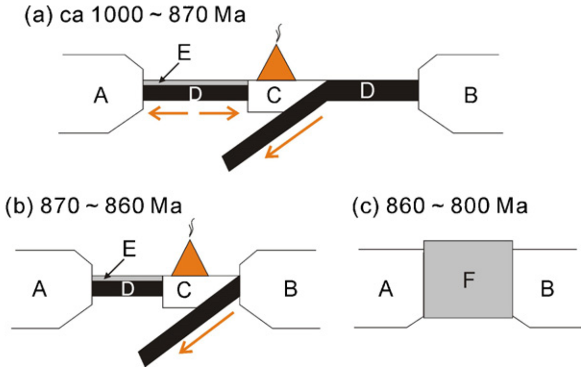

Fig. 6. Simplified model for the evolution of the Jiangnan orogen from ca. 1.0–0.8 Ga (modified after Cheng, 1991). (A) The Yangtze Block; (B) the Cathaysia Block; (C) the arc terrains resulted from the subduction; (D) the oceanic lithosphere; (E) the Precambrian basement sedimentary sequences; (F) the Jiangnan orogen.

Combined with the previously available geochemical and chronological data from the Jiangnan orogen, the new chronological data on the basement sedimentary sequences reveal a clear chronological framework for the evolution of the whole Jiangnan orogen (Fig. 6): (1) opening of the ocean basin and arc magmatism at ca. 1.0–0.87 Ga (Fig. 6a); (2) collision and high-pressure metamorphism at ca. 870–860 Ma (Fig. 6b); (3) jointing of the Yangtze and Cathaysia Blocks at 860–800 Ma (Fig. 6c). Moreover, it should be noted that the age gap between the basement strata and the overlying Banxi Group and its equivalent sequences might be very small, rather than extending from 1.0 Ga to ca. 0.8 Ga as suggested by Li et al. (2003b).

The available chronological data in the Jiangnan orogen indicate that the deposition of the basement sequences, the collisional events, the high-pressure metamorphism, the folding of the basement sedimentary rocks, the emplacement of peraluminous granites along the Jiangnan orogen, and the deposition of the overlying Neoproterozoic Danzhou/Banxi Group took place over a short period from 860–800 Ma. All of the geological events may have resulted from the formation and collapse of the Jiangnan orogen (Wang et al., 2004, 2006), the release of stress and/or energy, and the upwelling of deep mantle (not a typical mantle plume) following a long-lived subduction along the southeastern margin of the Yangtze Block.

6. Conclusions

The basement sedimentary rocks from the western part of the Jiangnan orogen have previously been regarded as Mesoproterozoic. However, our new LA-ICP–MS U–Pb dating results on detrital zircons from the rocks suggest that their maximum depositional age is ca. 860 Ma. There may be only a short hiatus between the basement sequences and the unconformably overlying Neoproterozoic strata (i.e. the Banxi Group and its equivalent sequences). The basement sequences were formed before the assembly of the Yangtze and Cathaysia and were then folded due to collision and related orogenic processes. Therefore, their maximum depositional age provides an upper age limit of ca. 860 Ma for the assembly of the two blocks. Combined with published chronological data for the igneous rocks along the Jiangnan orogen, it can be deduced that the Jinning orogeny along the southeastern margin of the Yangtze Block took place at 860–800 Ma, clearly younger than the typical Grenville-age orogeny. In view of the chronological results, the basement sequences shows similarities to the depositions in a foreland basin. The Yangtze Block and the arc terrains related to the subduction along the Jiangnan orogen may be the two main source regions for the basement sedimentary rocks.

Acknowledgements

This research was financially supported by National Natural Science Foundation of China (grants nos. 40221301 and 40572039) and ARC Discovery and Linkage International grants (SYO’R and WLG). Analytical data were obtained at GEMOC using instrumentation funded by ARC LIEF, and DEST Systemic Infrastructure Grants and Macquarie University. The manuscript benefited from the constructive comments of the two anonymous reviewers. We are grateful to N.J. Pearson, Suzy Elhlou and Eloise Beyer for their assistance with the analyses at GEMOC. Senior Engineers J.Z. Huang and X.S. Tang are thanked for their earnest direction and assistance on the field trip. The first author appreciates discussions with Prof. Jinhai Yu (NJU). This is contribution 486 from the ARC National Key Centre for Geochemical Evolution and Metallogeny of Continents (www.es.mq.edu.au/GEMOC).

References

Andersen, T., 2002. Correction of common Pb in U–Pb analyses that do not report ^{204}Pb. Chem. Geol. 192, 59–79.

BGMRGX (Bureau of Geology and Mineral Resources of Guangxi Province), 1985. Regional Geology of Guangxi Autonomous Region. Geological Publishing House, Beijing, pp. 38–40 (in Chinese with English abstract).

BGMRHN (Bureau of Geology and Mineral Resources of Hunan Province), 1988. Regional Geology of Hunan Province. Geological Publishing House, Beijing (in Chinese with English Abstract).

BGMRJX (Bureau of Geology and Mineral Resources of Guangxi Province), 1984. Regional Geology of Jiangxi Province. Geological Publishing House, Beijing (in Chinese with English abstract).

Black, L.P., Gulson, B.L., 1978. The age of the Mud Tank carbonatite, Strangways Range, Northern Territory. BMR J. Aust. Geol. Geophys. 3, 227–232.

Charvet, J., Shu, L.S., Shi, Y.S., Guo, L.Z., Faure, M., 1996. The building of South China: collision of Yangtze and Cathaysia blocks, problems and tentative answers. J. Southeast Asian Earth Sci. 13, 223–235.

Chen, J.F., Foland, K.A., Xing, F.M., Xu, X., Zhou, T.X., 1991. Magmatism along the southeast margin of the Yangtze Block: Precambrian collision of the Yangtze and Cathaysia Blocks of China. Geology 19, 815–818.

Cheng, H., 1991. The late Proterozoic collision orogen in Northwestern Zhejiang Province. Geol. Rev. 37 (3), 203–213 (in Chinese with English abstract).

Cheng, H., 1993. Geochemistry of Proterozoic island-arc volcanic rocks in northwest Zhejiang. Geochimica 1, 18–27 (in Chinese with English abstract).

Condie, K.C., 2002. The supercontinent cycle: are there two patterns of cyclicity? J. Afr. Earth Sci. 35, 179–183.

Fedo, C.M., Sircombe, K.N., Rainbird, R.H., 2003. Detrital zircon analysis of the sedimentary record. Rev. Miner. Geochem. 53, 277–304.

Gan, X.C., Zhao, F.Q., Jin, W.S., Jin, D.Z., 1996. The U–Pb ages of early Proterozoic–Archean zircons captured by igneous rocks in Southern China. Geochimica 25 (2), 112–120 (in Chinese with English abstract).

Greentree, M.R., Li, Z.X., Li, X.H., Wu, H.C., 2006. Late Mesoproterozoic to earliest Neoproterozoic basin record of the Sibao orogenesis in western South China and relationship to the assembly of Rodinia. Precambrian Res. 151, 79–100.

Griffin, W.L., Belousova, E.A., Shee, S.R., Pearson, N.J., O'Reilly, S.Y., 2004. Archean crustal evolution in the northern Yilgarn Craton: U–Pb and Hf-isotope evidence from detrital zircons. Precambrian Res. 131, 231–282.

Guo, L.Z., Shi, Y.S., Ma, R.S., 1980. The geotectonic framework and crustal evolution of South China. In: Scicentific Paper on Geology for International Exchange. J. Geological Publishing House, Beijing, pp. 109–116 (in Chinese with English abstract).

GXRGST (Guangxi Regional Geological Survey Team), 1995. Regional Geological Survey Report (Sanfang area, 1:50000) (in Chinese).

Han, F., Shen, J.Z., Nie, F.J., Ding, X.S., Li, S.C., Yang, K.T., Yang, C., 1994. The geochronological studies of Sibao group in the southern margin of Jiangnan massif. Acta Geosci. Sinica 1/2, 43–50 (in Chinese with English abstract).

Hoffman, P.F., Kaufmann, A.J., Halverson, G.P., Schrag, D.P., 1998. A Neoproterozoic snowball Earth. Science 281, 1342–1346.

Hsü, K., Sun, S., Li, J., Chen, H., Pen, H., Sengor, A., 1988. Mesozoic overthrust tectonics in South China. Geology 16, 418–421.

Hu, S.L., Zou, H.B., Zhou, X.M., 1993. $^{40}Ar/^{39}Ar$ ages of the muscovites of Shexian cordierite-bearing granites of Anhui Province and the crossite for the Dexing albite granites of Jiangxi Province: tectonic implications. In: Li, J.L. (Ed.), Lithospheric Structures and Geological Evolution in Continent from Southeastern China. Metallurgical Industry Press, Beijing, pp. 141–169 (in Chinese).

Jackson, S.E., Pearson, N.J., Griffin, W.L., Belousova, E.A., 2004. The application of laser ablation-inductively coupled plasma–mass spectrometry to in situ U–Pb zircon geochronology. Chem. Geol. 211, 47–69.

Li, W.X., Li, X.H., Li, Z.X., 2005. Neoproterozoic bimodal magmatism in the Cathaysia Block of South China and its tectonic significance. Precambrian Res. 136, 51–66.

Li, X.H., 1999. U–Pb zircon ages of granites from the southern margin of the Yangtze margin: timing of Neoproterozoic Jinning Orogen in SE China and implication for Rodinia assembly. Precambrian Res. 97, 43–57.

Li, X.H., Li, Z.X., Ge, W.C., Zhou, H.W., Li, W.X., Liu, Y., Wingate, M.T.D., 2003a. Neoproterozoic granitoids in South China: crustal melting above a mantle plume at ca. 825Ma? Precambrian Res. 122, 45–83.

Li, X.H., Zhao, Z.H., Gui, X.T., Yu, J.S., 1991. Sm-Nd isotopic and zircon U–Pb constraints on the age of formation of the Precambrian crust in Southeast China. Geochimica 3, 255–264 (in Chinese with English abstract).

Li, X.H., Zhou, G.Q., Zhao, J.X., Fanning, C.M., Compston, W., 1994. SHRIMP ion microprobe zircon U–Pb age and Sm–Nd isotopic characteristics of the NE Jiangxi ophiolite and its tectonic implications. Chin. J. Geochem. 13, 317–325.

Li, Z.X., Li, X.H., Kinny, P.D., Wang, J., 1999. The breakup of Rodinia: did it start with a mantle plume beneath South China? Earth Planet. Sci. Lett. 173, 171–181.

Li, Z.X., Li, X.H., Zhou, H.W., Kinny, P.D., 2002. Grenvillian continental collision in south China: new SHRIMP U–Pb zircon results and implications for the configuration of Rodinia. Geology 30, 163–166.

Li, Z.X., Li, X.H., Kinny, P.D., Wang, J., Zhang, S., Zhou, H.W., 2003b. Geochronology of Neoproterozoic syn-rift magmatism in the Yangtze Craton, South China and correlations with other continents: evidence for a mantle superplume that broke up Rodinia. Precambrian Res. 122, 85–109.

Ludwig, K.R., 1999. User's Manual for Isoplot/Ex Version 2.06: a Geochronological Toolkit for Microsoft Excel, vol. 1a (Special Publication). Geochronology Center, Berkeley, pp. 1–49.

McLelland, J., Daly, J.S., McLelland, J.M., 1996. The Grenville Orogenic Cycle (ca. 1350–1000 Ma): an Adiron-dack perspective. Tectonophysics 265, 1–28.

Meert, J.G., Powell, C.McA., 2001. Assembly and break-up of Rodinia: introduction to the special volume. Precambrian Res. 110, 1–8.

Meert, J.G., Torsvik, T.H., 2003. The making and unmaking of a supercontinent: Rodinia revisited. Tectonophysics 375, 261–288.

Nelson, D.R., 2001. An assessment of the determination of depositional ages for Precambrian clastic sedimentary rocks by U–Pb dating of detrital zircons. Sedimen. Geol. 141/142, 37–60.

Shu, L.S., Zhou, G.Q., Shi, Y.S., Yin, J., 1993. Study of high pressure metamorphic blueschist and its late Proterozoic age in the eastern Jiangnan belt. Chin. Sci. Bull. 38, 1779–1882 (in Chinese).

Shu, L.S., Shi, Y.S., Guo, L.Z., Charvet, J., Sun, Y. (Eds.), 1995. Plate Tectonic Evolution and the Kinematics of Collisional Orogeny in the Middle Jiangnan, Eastern China, vol. 5/6. Nanjing University Publ. (in Chinese with English abstract).

Tang, X.S., 1989. Lithostratigraphic study of Lengjiaxi Group in Hunan. Hunan Geol. 8 (2), 1–9 (in Chinese with English abstract).

Tang, X.S., Huang, J.Z., Guo, L.Q., 1997. Hunan Banxi Group and its tectonic environment. Hunan Geol. 16, 219–226 (in Chinese with English abstract).

Torsvik, T.H., 2003. The Rodinia jigsaw puzzle. Science 300, 1379–1381.

van Achterbergh, E., Ryan, C., Jackson, S., Griffin, W., 2001. In: Sylvester, P. (Ed.), Appendix 3 Data Reduction Software for LA-ICP–MS in "Laser-Ablation-ICPMS in the Earth Sciences", 29.

Mineralogical Association of Canada Short Course, pp. 239–243.

Wang, D.Z., 2004. The study of Granitic Rocks in South China: looking back and forward. Geol. J. China Univ. 10 (3), 305–314 (in Chinese with English abstract).

Wang, J., 2000. Neoproterozoic Rifting History of South China: Significance to Rodinia Breakup. Geological Publishing House, Beijing (in Chinese with English abstract).

Wang, J., Li, X.H., Duan, T.Z., Liu, D.Y., Song, B., Li, Z.X., Gao, Y.H., 2003. Zircon SHRIMP U–Pb dating for the Cangshuipu volcanic rocks and its implications for the lower boundary age of the Nanhua strata in South China. Chin. Sci. Bull. 48, 1663–1669.

Wang, J., Li, Z.X., 2003. History of Neoproterozoic rift basins in South China: implications for Rodinia breakup. Precambrian Res. 122, 141–158.

Wang, X.L., Zhou, J.C., Qiu, J.S., Gao, J.F., 2004. Geochemistry of the Meso- to Neoproterozoic basic-acid rocks from Hunan Province, South China: implications for the evolution of the western Jiangnan orogen. Precambrian Res. 135, 79–103.

Wang, X.L., Zhou, J.C., Qiu, J.S., Zhang, W.L., Liu, X.M., Zhang, G.L., 2006. LA-ICPMS U–Pb zircon geochronology of the Neoproterozoic igneous rocks from Northern Guangxi, South China: implications for petrogenesis and tectonic evolution. Precambrian Res. 145, 111–130.

Wang, X.L., Zhou, J.C., Qiu, J.S., Jiang, S.Y., Shi, Y.R., in press. Geochronology and geochemistry of Neoproterozoic mafic rocks from western Hunan, South China: implications for petrogenesis and post-orogenic extension. Geol. Mag.

Wiedenbeck, M., Alle, P., Corfu, F., Griffin, W.L., Meier, M., Oberli, F., von Quadt, A., Roddick, J.C., Spiegel, W., 1995. Three natural zircon standards for U–Th–Pb, Lu–Hf, trace element and REE analyses. Geostand. Newslett. 19, 1–23.

Wu, R.X., Zheng, Y.F., Wu, Y.B., Zhao, Z.F., Zhang, S.B., Liu, X.M., Wu, F.Y., 2006. Reworking of juvenile crust: Element and isotope evidence from Neoproterozoic granodiorite in South China. Precambrian Res. 146, 179–212.

Xing, F.M., Xu, X., Chen, J.F., Zhou, T.X., Foland, K.A., 1992. The late Proterozoic continental accretionary history of the southeastern margin of the Yangtze platform. Acta Geol. Sinica 66, 59–71 (in Chinese with English abstract).

Xu, D.R., Gu, X.X., Li, P.C., Chen, G.H., Xia, B., Bachlinski, R., He, Z.L., Fu, G.G., 2007. Mesoproterozoic–Neoproterozoic transition: Geochemistry, provenance and tectonic setting of clastic sedimentary rocks on the SE margin of the Yangtze Block, South China. J. Asian Earth Sci. 29, 637–650.

Ye, M.F., Li, X.H., Li, W.X., Liu, Y., Li, Z.X., 2007. SHRIMP zircon U–Pb geochronological and whole-rock geochemical evidence for an early Neoproterozoic Sibaoan magmatic arc along the southeastern margin of the Yangtze Block. Gondwana Res. 12, 144–156.

Yuan, H.L., Wu, F.Y., Gao, S., Liu, X.M., Xu, P., Sun, D.Y., 2003. Determination of U–Pb age and rare earth element concentrations of zircons from Cenozoic intrusions in northeastern China by laser ablation ICP–MS. Chin. Sci. Bull. 48, 2411–2421.

Zhang, G.L., 2004. Kinematics and Dynamics of pre-Devonian tectonic evolution at South Margin of Yangtze Block in North Guangxi. Ph.D. Thesis. Central South University, pp. 122–123 (in Chinese with English abstract).

Zhao, G.C., Cawood, P.A., 1999. Tectonothermal evolution of the Mayuan assemblage in the Cathaysia Block: implications for Neoproterozoic collision-related assembly of the South China craton. Am. J. Sci. 299, 309–339.

Zhong, Y.F., Ma, C.Q., She, Z.B., Lin, G.C., Xu, H.J., Wang, R.J., Yang, K.G., Liu, Q., 2005. SHRIMP U–Pb zircon geochronology of the Jiuling granitic complex batholith in Jiangxi Province. Earth Sci.—J. China Univ. Geosci. 30 (6), 685–691 (in Chinese with English abstract).

Zhou, J.C., Wang, X.L., Qiu, J.S., Gao, J.F., 2004. Geochemistry of Meso- and Neoproterozoic mafic–ultramafic rocks from northern Guangxi, China: arc or plume magmatism? Geochem. J. 38, 139–152.

Zhou, M.F., Yan, D.P., kennedy, A.K., Li, Y.Q., Ding, J., 2002. SHRIMP U–Pb zircon geochronological and geochemical evidence for Neoproterozoic arc-magmatism along the western margin of the Yangtze Block, South China. Earth Planet. Sci. Lett. 196, 51–67.

Zhou, X.M., 2003. My thinking about granite geneses of South China. Geol. J. China Univ. 9 (4), 556–565 (in Chinese with English abstract).

Zhou, X.M., Wang, D.Z., 1988. The peraluminous granodiorites with low initial 87Sr/86Sr ratio and their genesis in southern Anhui province, eastern China. Acta Petrol. Sinica 4 (3), 37–45 (in Chinese with English abstract).

Zhou, X.M., Zhu, Y.H., 1993. Late Proterozoic collisional orogen and geosuture in southeastern China: Petrological evidences. Chin. J. Geochem. 12 (3), 239–251.